

www.crt-journal.org

Crystal Research and Technology

Journal of Experimental and Industrial Crystallography

Zeitschrift für experimentelle und technische Kristallographie

РЕПОЗИТОРИЙ БГУ

WILEY-VCH

REPRINT

$T(x)$ phase diagram of the CuSbS_2 – CuInS_2 system and solubility limit of Sb in CuInS_2

B. V. Korzun^{*1}, A. N. Gavrilenko², A. A. Fadzeyeva¹, O. V. Ignatenko¹, I. I. Maroz¹, V. R. Sobol³, M. Rusu⁴, R. Klenk⁴, C. Merschjann⁴, Th. Schedel-Niedrig⁴, and M. Ch. Lux-Steiner⁴

¹ State Scientific and Production Association “Scientific-Practical Materials Research Centre of the National Academy of Sciences of Belarus”, P. Brovki 19, Minsk 220072, Belarus

² Kazan State Power University, Krasnoselskaya 51, Kazan 420066, Russia

³ Belarus State Pedagogical University, Sovetskaya 6, Minsk 220050, Belarus

⁴ Helmholtz Zentrum Berlin für Materialien und Energie, Hahn-Meitner Platz 1, 14109 Berlin, Germany

Received 24 July 2013, revised 24 July 2013, accepted 5 August 2013

Published online 26 August 2013

Key words CuInS_2 , CuSbS_2 , $T(x)$ phase diagram, solubility.

The starting ternary compounds CuInS_2 and CuSbS_2 and alloys of the CuSbS_2 – CuInS_2 system with the molar fractions of CuInS_2 (x) equal to 0.05, 0.15, 0.25, 0.375, 0.50, 0.625, 0.75, 0.85, and 0.95 were prepared and the phase relations in this system were investigated by X-ray powder diffraction, optical microscopy, scanning electron microscopy, and differential thermal analysis. It was shown that the T – x phase diagram of the CuInS_2 – CuSbS_2 system has a eutectic character with the eutectic temperature of 807 K. The alloys of the CuSbS_2 – CuInS_2 system with the molar fraction of CuInS_2 in the range from 0.038 to 0.941 at room temperature are two-phased, and the limits of solubility are 0.059 molar fractions for CuSbS_2 in CuInS_2 and 0.038 molar fractions for CuInS_2 in CuSbS_2 .

© 2013 WILEY-VCH Verlag GmbH & Co. KGaA, Weinheim

1 Introduction

One of the most promising materials of the I–III–VI₂ group semiconductors is copper indium disulfide (CuInS_2). Initially studied as an electroluminescent material [1], CuInS_2 then received significant attention as a solar cell material. The thin-film absorber preparation by coevaporation of the elements on Mo-coated glass substrates leading to a solar cell with 11.4% efficiency was described [2] and pilot production of the large-area CuInS_2 -based cells has been developed [3]. The overviews of the current state of scientific understanding and technological development of solar cells based on CuInS_2 are presented in [4,5]. It was shown that in order to adjust the physical properties of CuInS_2 , it is necessary to optimize the technology of doping of this material. Chemical elements of the V-th group As, Sb, Bi can be used as such doping elements. The diffusion of Sb into CuInS_2 films has been examined by XPS, SIMS, and electrical measurements [6]. The results suggest that Sb acts as a compensating donor and can be used to drive the junction away from the heterointerface. It was also found that p-type CuInS_2 crystals could be grown by the hot-press method in the range 673–973 K for 1 h under pressures of 10–100 MPa from Cu_2S , In_2S_3 , and Sb powders [7]. It was suggested that the Sb atoms in the S site might enhance the p-type conductivity. To determine the limits of solid solubility of Sb in the CuInS_2 ternary compound, it is necessary to study the phase relations in the CuInS_2 – CuSbS_2 system.

The special feature of this system is that it is formed by two compounds which have analogs among minerals – roquesite (CuInS_2) and chalcostibite (CuSbS_2). CuInS_2 is studied actively and it was shown from quenching experiments followed by X-ray analysis that its region of existence is very small and in fact is limited to $0 < x < 0.05$ in $\text{Cu}_{1-x}\text{In}_{1+x/3}\text{S}_2$ [8], or situated in the range composition 50–52 mol.% of In_2S_3 in the Cu_2S – In_2S_3 system [9]. The T – x phase diagram of the Cu_2S – In_2S_3 pseudobinary system has been determined by differential thermal analysis and X-ray diffraction [9,10]. It appears that CuInS_2 exists in three modifications, (i) up to 1253 K

*Corresponding author: e-mail: korzun@physics.by

in the chalcopyrite structure, (ii) between 1253 and 1318 K in the zincblende structure, (iii) and above 1318 K up to the melting point at 1363 K, in a still unknown structure, which tentatively is assumed to be wurtzite [9]. Study of the phase diagrams of the Cu_2S – In_2S_3 and CuS – InS pseudobinary systems showed a homogeneity region for CuInS_2 at room temperature ranging from 2 mol.% in the In_2S_3 direction to 1.5 mol.% in the CuS direction [10].

Knowledge of CuSbS_2 is rather scarce and contradictory. CuSbS_2 is reported to crystallize in the space group Pnam with 6.016, 3.796, and 14.49 Å for the lattice constants a , b and c , respectively [11]. Investigations of the Cu_2S – Sb_2S_3 pseudobinary system showed that there is only one ternary compound with the chemical composition corresponding to CuSbS_2 in this system [12,13]. It melts congruently with the melting point of 825 [12], 819 [14] or 808 K [15]. The heat of melting is 19.4 [14] or 8.00 kcal/mol [15].

The aim of the present paper is to study the phase relations in the CuSbS_2 – CuInS_2 system by X-ray powder diffraction (XRPD), optical microscopy, scanning electron microscopy (SEM), and differential thermal analysis (DTA). Furthermore, it will be of interest to determine the limit of solubility of Sb in CuInS_2 .

2 Experimental

The initial elements for the preparation of the CuSbS_2 and CuInS_2 ternary compounds and their alloys were 99.9998% copper, 99.9997% indium, 99.999% antimony, and 99.9999% sulfur. The starting ternary compounds and nine alloys of the CuInS_2 – CuSbS_2 system with the molar fractions of CuInS_2 (x) equal to 0.05, 0.15, 0.25, 0.375, 0.50, 0.625, 0.75, 0.85, and 0.95 were prepared in evacuated and closed quartz ampoules by reaction of the elements at elevated temperatures. To obtain samples by melting, the mixtures of the chemical elements were heated up to 1393 K, exceeding the melting point of CuInS_2 by 30 K, and maintained at this temperature for 2 hours. Then, the samples were cooled down to room temperature at a rate of 3–5 K/min. To homogenize the product, the subsequent annealing was carried out at 683 K for 550 hours.

The phase relations in the CuSbS_2 – CuInS_2 system were investigated by means of X-ray powder diffraction (Cu K_α -radiation, 1.5406 Å), optical microscopy (microscope MIM 7), scanning electron microscopy (electron microscope Jeol, equipped with an energy-dispersive X-ray detector, EDX), and differential thermal analysis (laboratory apparatus).

The DTA measurements were performed using special carriers within a high-temperature steel clamp. The temperatures of the structural phase transitions were determined using Pt/90%Pt-10%Rh thermocouples with heating rates being 2–3 K/min (accuracy of ± 2 K). Reproducible results were obtained by placing powder samples of 1 g in evacuated ($1.3 \cdot 10^{-2}$ Pa) quartz capsules using Al_2O_3 as a reference material. The temperature calibration of the apparatus was achieved by recording solid-state phase transitions and melting of K_2SO_4 (858 and 1342 K), NaCl (1074 K), and Na_2SO_4 (1157 K).

3 Results and discussion

The XRPD data show that most of the prepared alloys of the CuSbS_2 – CuInS_2 system consist of two phases (figure 1). In figure 1 the Bragg peaks of the phase with the chalcopyrite structure are denoted by symbol * and the Bragg peaks of the phase with the chalcostibite structure are denoted by symbol o. CuInS_2 crystallizes in the tetragonal structure with the lattice constants 5.523 and 11.13 Å for a and c , respectively. CuSbS_2 crystallizes in the orthorhombic structure with the lattice constants 6.015, 3.792, and 14.464 Å for a , b and c , respectively. From XRPD results it can be concluded that the solubility of CuInS_2 in CuSbS_2 and CuSbS_2 in CuInS_2 does not exceed 0.05 molar fractions of the ternary compound.

The microstructure studies using optical microscope (figure 2a, b) and scanning electron microscope (figure 2c) confirmed the absence of the formation of complete solid solutions in the CuSbS_2 – CuInS_2 system. Crystals based on the compound with a higher melting point (CuInS_2), which crystallize first, grow in liquids until they coalesce. The primary crystals with the chalcopyrite structure based on the CuInS_2 ternary compound crystallize in a regular form. The regularity of crystallographic forms is detected as dendrites in figure 2a, b (grains of black colour). When the content of CuInS_2 increases these primary crystals are completely growing together and a phase based on CuSbS_2 is detected as irregular inclusions (figure 2c, black colour).

The results of the determination of the chemical composition of these two phases are presented in table 1. They indicate that the alloys of the CuSbS_2 – CuInS_2 system with the molar fraction of CuInS_2 in the range from

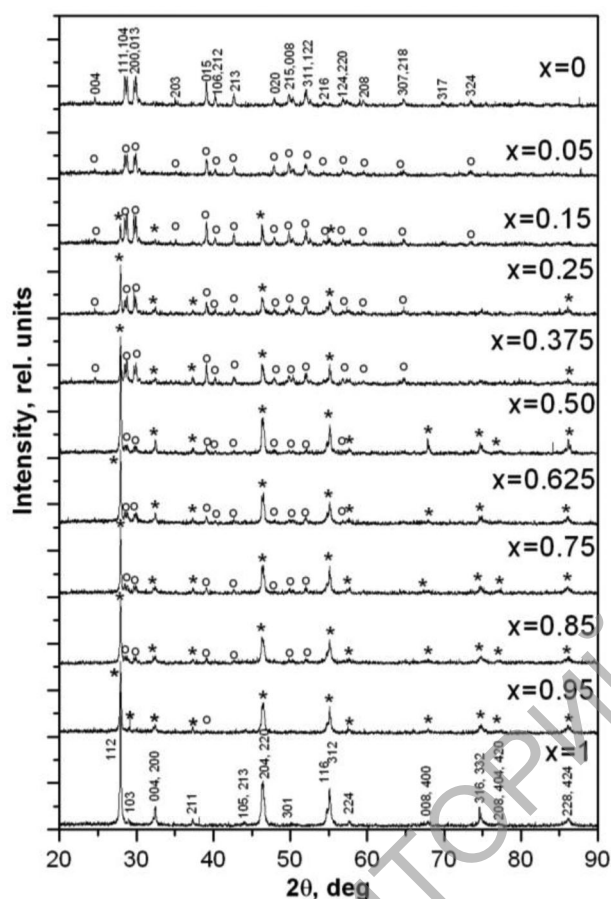


Fig. 1 XRPD patterns at room temperature for CuInS_2 ($x = 1$), CuSbS_2 ($x = 0$), and alloys of the CuSbS_2 – CuInS_2 system. The denotation of XRPD patterns for alloys corresponds to their initial composition, expressed in molar fractions of CuInS_2 .

Table 1 Chemical composition of different alloys of the CuSbS_2 – CuInS_2 system, determined from EDX measurements.

Initial composition	Phase with the chalcopyrite structure	Phase with the chalcostibite structure
CuSbS_2		$\text{CuSb}_{0.928}\text{S}_{1.764}$
$\text{CuIn}_{0.15}\text{Sb}_{0.85}\text{S}_2$	$\text{CuIn}_{0.888}\text{Sb}_{0.056}\text{S}_{1.894}$	$\text{CuIn}_{0.038}\text{Sb}_{0.983}\text{S}_{1.919}$
$\text{CuIn}_{0.50}\text{Sb}_{0.50}\text{S}_2$	$\text{CuIn}_{0.928}\text{Sb}_{0.058}\text{S}_{1.979}$	$\text{CuIn}_{0.046}\text{Sb}_{0.944}\text{S}_{1.934}$
$\text{CuIn}_{0.85}\text{Sb}_{0.15}\text{S}_2$	$\text{CuIn}_{0.980}\text{Sb}_{0.064}\text{S}_{1.995}$	$\text{CuIn}_{0.031}\text{Sb}_{0.960}\text{S}_{1.834}$

0.038 to 0.941 at room temperature consist of two phases. Thus, the limits of solubility are 0.059 molar fractions for CuSbS_2 in CuInS_2 and 0.038 molar fractions for CuInS_2 in CuSbS_2 .

Figure 3 shows the DTA heating and cooling curves of the alloys of the CuInS_2 – CuSbS_2 system. The behavior of CuSbS_2 during cooling shows that for this compound a supercooling is characteristic and crystallization occurs at the eutectic temperature of the Cu_2S – Sb_2S_3 system at 750 K. It proves that the homogeneous composition does not correspond to the stoichiometric composition of CuSbS_2 , as was previously argued [12–14], and shifts towards the Sb_2S_3 binary compound. As seen on the other thermograms, the thermal peak denoted as 1 is also caused by this fact, namely, the displacement of the homogeneous composition from the stoichiometric composition CuSbS_2 and the beginning of melting (or end of crystallization) at the eutectic temperature in the Cu_2S – Sb_2S_3 system at 750 K.

The thermal peak denoted as 2 and occurring at 807 K corresponds to the eutectic horizontal in the CuSbS_2 – CuInS_2 system as it arises at the temperature lower than the melting point of the low-melted compound in this

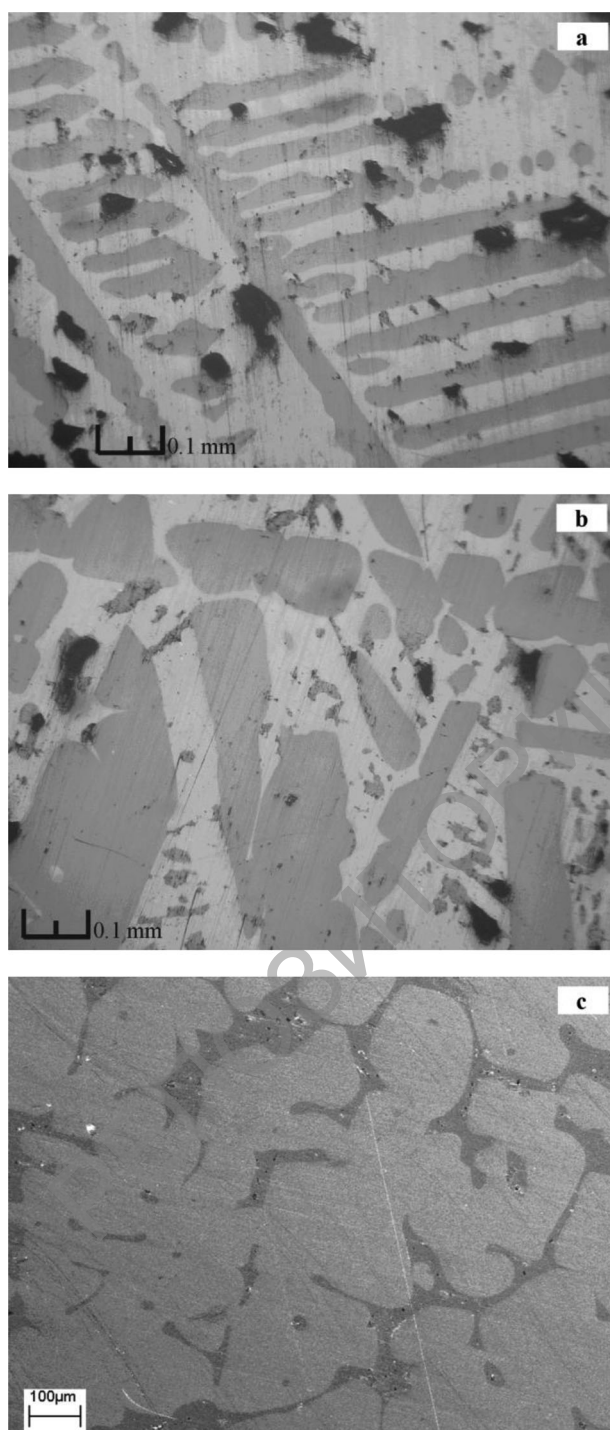


Fig. 2 Microstructure of alloys of the CuSbS_2 – CuInS_2 system with $x = 0.15$ (a), 0.50 (b), and 0.85 (c) molar fractions of CuInS_2 .

system CuSbS_2 (823 K). The composition of the eutectics is not determined but can not exceed 0.05 molar fractions of CuInS_2 . Since melting of alloys of this system takes place over a temperature range of 400 K for the CuInS_2 -rich alloys, the end of melting is displayed by an additional endothermic peak denoted on the thermograms as 3.

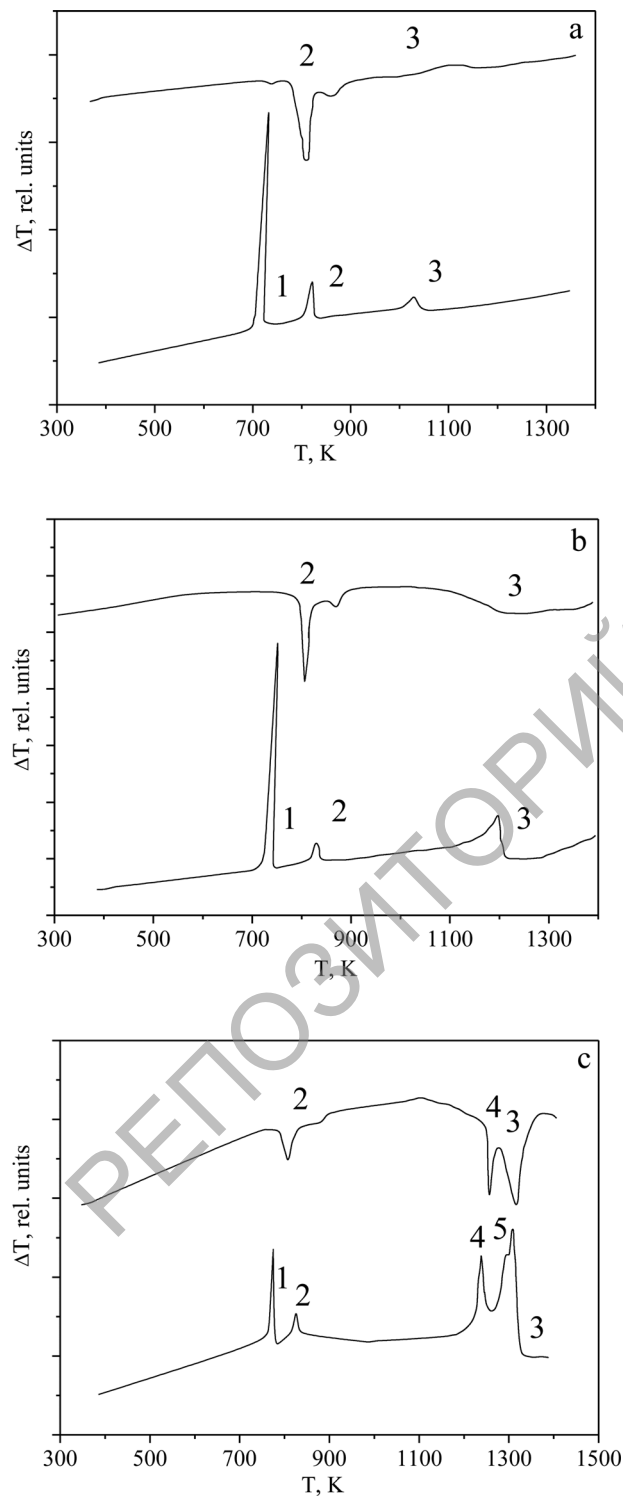


Fig. 3 DTA heating (top) and cooling (bottom) curves of alloys of the $\text{CuSbS}_2\text{-CuInS}_2$ system with $x = 0.15$ (a), 0.50 (b), and 0.85 (c) molar fractions of CuInS_2 .

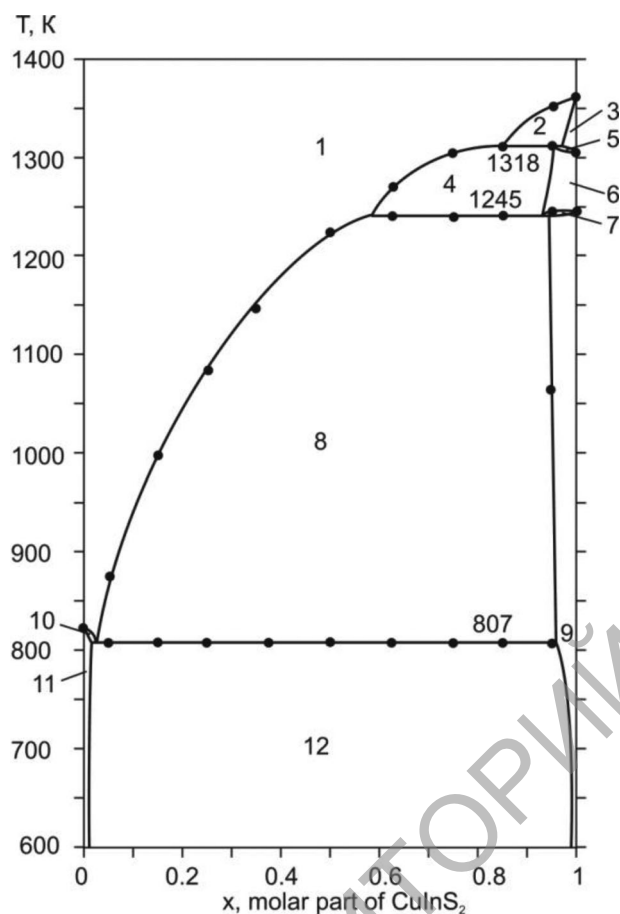


Fig. 4 T-x phase diagram of the $\text{CuSbS}_2\text{-CuInS}_2$ system. Numbers denote the phase fields: 1: L, 2: $L + \gamma$, 3: γ , 4: $L + \beta$, 5: $\gamma + \beta$, 6: β , 7: $\beta + \alpha$, 8: $L + \alpha$, 9: α , 10: $L + \delta$, 11: δ , 12: $\alpha + \delta$. Here, L is liquid, γ is a presumably phase with the wurtzite structure, β is a phase with the sphalerite structure, α is a phase with the chalcopyrite structure, and δ is a phase with the chalcostibite structure.

The existence of CuInS_2 in three polymorphic modifications leads to further complication of interactions in this system. In addition to the thermal effect of melting, at high temperatures the thermograms of the alloys based on the CuInS_2 ternary compound have two thermal peaks caused by the polymorphous transformations (figure 3c). The thermal peak 4 is caused by a structural phase transition from the tetragonal chalcopyrite structure to the cubic sphalerite structure (zinc blend structure).

The nature of the second polymorphic transformation is presumably a phase transition from the sphalerite structure to the wurtzite structure (SG $P6_3mc$). This second phase transition for the alloy with the initial composition $\text{CuIn}_{0.85}\text{Sb}_{0.15}\text{S}_2$ (figure 3c) is shown only on the cooling curve and denoted as 5. The T-x phase diagram of the $\text{CuSbS}_2\text{-CuInS}_2$ system has the eutectic character, where the temperature of the eutectic is 807 K (figure 4). Taking into account the results of XRPD, the microstructure investigations, and DTA, it can be concluded that the alloys of the $\text{CuSbS}_2\text{-CuInS}_2$ system with the molar fraction of CuInS_2 in the range from 0.038 to 0.941 at room temperature consist of two phases, and the limits of the solubility are 0.059 molar fractions for CuSbS_2 in CuInS_2 and 0.038 molar fractions for CuInS_2 in CuSbS_2 .

The transitions from the chalcopyrite structure to the sphalerite structure and from the chalcopyrite structure to the presumably wurtzite structure for the CuInS_2 ternary compound are not connected with the existence of the two-phase region and are direct transitions. For the alloys of the $\text{CuSbS}_2\text{-CuInS}_2$ system these transitions occur through the temperature interval of coexistence of two phases, with the chalcopyrite structure and the sphalerite structure (field 7 of T-x phase diagram, figure 4) and with the sphalerite structure and presumably the wurtzite structure (field 5). The analogous behaviour, namely, coexistence of two phases (chalcopyrite and sphalerite), has

been also discovered for the $\text{CuInS}_{2x}\text{Se}_{2(1-x)}$ solid solutions in the whole range of compositions excluding pure phases CuInS_2 and CuInSe_2 [16]. The line of polymorphic transformation from the chalcopyrite structure to the sphalerite structure is situated at 1245 K and the line of polymorphic transformation from the sphalerite structure to the presumably wurtzite structure is situated at 1318 K (figure 4).

It is also noteworthy that the covalent atomic radii for In and Sb are similar and equivalent to 0.142(5) and 0.139(5) nm, respectively [17]. Ionic radii of In and Sb are also similar – 0.080 and 0.076 nm for In^{+3} and Sb^{+3} ions, respectively [18]. This contributes to the formation of complete series of solid solutions in this system formed by the two ternary compounds with covalent (or covalent-ionic) chemical bond. The electronegativities of In and Sb differ and have values 1.78 and 2.05, respectively [19]. Taking into account that the electronegativity of S atoms is 2.58 [19], the electronegativity difference between two atoms is 0.77 and 0.59 for the In – S and Sb – S bond, respectively. Thus, with the replacement of In by Sb, there is a decrease of the difference in electronegativity between two atoms forming chemical bonds (In and S or Sb and S). In general, with a decrease of the electronegativity difference between two atoms, the more polar bond is the one formed between the atoms, where the atom with the lower electronegativity is at the positive end of the dipole. Covalent bond In – S, in comparison to the covalent bond Sb – S, is more ionic. As a result, the starting compounds CuInS_2 and CuSbS_2 crystallize in different crystal structures. The crystal structure of CuInS_2 is unstable for the alloys with the In – Sb substitution and these alloys consist of two phases. This is also valid for the Sb – In substitution, when the crystal structure of CuSbS_2 is becoming unstable and the alloys also become two-phased.

4 Conclusions

The CuSbS_2 and CuInS_2 ternary compounds and alloys of the CuSbS_2 – CuInS_2 system with the molar fractions of CuInS_2 (x) equal to 0.05, 0.15, 0.25, 0.375, 0.50, 0.625, 0.75, 0.85, and 0.95 were prepared. The phase relations in this system were investigated using X-ray powder diffraction, differential thermal analysis, optical microscopy, and scanning electron microscopy, equipped with an energy-dispersive X-ray detector. It was established that the T – x phase diagram of the CuSbS_2 – CuInS_2 system has a eutectic character with the eutectic temperature of 807 K, the composition of the eutectics is not determined but can not exceed 0.05 molar fractions of CuInS_2 . The alloys of the CuSbS_2 – CuInS_2 system with the molar fractions of CuInS_2 in the range from 0.038 to 0.941 at room temperature consist of the two phases. The limits of solubility are 0.059 molar fractions for CuSbS_2 in CuInS_2 and 0.038 molar fractions for CuInS_2 in CuSbS_2 .

Acknowledgements It is a pleasure to thank Prof. Dr. S. Fiechter for helpful discussion and Ms. C. Kelch for fruitful help with the SEM studies (both Helmholtz Zentrum Berlin für Materialien und Energie, Berlin, Germany). The partial financial support from the Belarusian Republican Foundation for Fundamental Research (grant No. $\Phi 06$ –166) is greatly appreciated.

References

- [1] P. M. Bridenbaugh and P. Migliorato, *Appl. Phys. Lett.* **26**, 459 (1975).
- [2] K. Siemer, J. Klaer, I. Luck, J. Bruns, R. Klenk, and D. Bräunig, *Sol. Energ. Mat. Sol. Cells* **67**, 159 (2001).
- [3] N. Meyer, A. Meeder, and D. Schmid, *Thin Solid Films* **515**, 5979 (2007).
- [4] R. Klenk, J. Klaer, R. Scheer, M. Ch. Lux-Steiner, I. Luck, N. Meyer, and U. Ruhle, *Thin Solid Films* **480–481**, 509 (2005).
- [5] R. Klenk, J. Klaer, C. Köble, R. Mainz, S. Merdes, H. Rodriguez-Alvarez, R. Scheer, and H.W. Schock, *Sol. Energ. Mat. Sol. Cells* **95**, 1441 (2011).
- [6] I. Hengel, R. Klenk, E. Garcia Villora, and M.-Ch. Lux-Steiner, 2nd World Conference and Exhibition on Photovoltaic Solar Energy Conversion (6–10 July, 1998, Vienna, Austria) 546 (1998).
- [7] H. Komaki, K. Yoshino, Y. Akaki, M. Yoneta, and T. Ikari, *Phys. Stat. Sol. (c)* **0**, 759 (2003).
- [8] A. W. Verheijen, L. J. Giling, and J. Bloem, *Mater. Res. Bull.* **14**, 237 (1979).
- [9] J. J. M. Binsma, L. J. Giling, and J. Bloem, *J. Cryst. Growth* **50**, 429 (1980).
- [10] S. Fiechter, Y. Tomm, M. Kanis, R. Scheer, and W. Kanetek, *Phys. St. Sol. (b)* **245**, 1761 (2008).
- [11] M. F. Razmara, C. M. B. Henderson, R. A. D. Patrick, A. M. T. Bell, and J. M. Charnock, *Mineral. Mag.* **61**, 79 (1979).
- [12] R. A. Kuliev, A. N. Krestovnikov, and V. M. Glazov, *Zhurnal fizicheskoi khimii* **XLIII**, 3063 (1969).
- [13] R. A. Kuliev, A. N. Krestovnikov, and V. M. Glazov, *Neorganicheskie materialy* **5**, 2233 (1969).
- [14] V. M. Glazov, R. A. Kuliev, and A. N. Krestovnikov, *Neorganicheskie materialy* **6**, 2194 (1970).

- [15] R. Blachnik and B. Gather, *Z. Naturforschung* **27B**, 1417 (1972).
- [16] I. V. Bodnar and B. V. Korzun, *Mater. Res. Bull.* **18**, 519 (1983).
- [17] B. Cordero, V. Gomez, A. E. Platero-Prats, M. Reves, J. Echeverria, E. Cremades, F. Barragan, and S. Alvarez, *Dalton Trans.* 2832 (2008).
- [18] L. Pauling, *The Nature of the Chemical Bond*, Cornell University Press, Ithaca 1980.
- [19] R. D. Shannon, *Acta Cryst.* **A32**, 751 (1976).

РЕПОЗИТОРИЙ БГПУ